



# Exceptional resistance to grain growth in nanocrystalline CoCrFeNi high entropy alloy at high homologous temperatures



S. Praveen <sup>a</sup>, Joysurya Basu <sup>b</sup>, Sanjay Kashyap <sup>c</sup>, Ravi Sankar Kottada <sup>a,\*</sup>

<sup>a</sup> Department of Metallurgical and Materials Engineering, Indian Institute of Technology Madras, Chennai, India

<sup>b</sup> Physical Metallurgy Group, Indira Gandhi Centre for Atomic Research, Kalpakkam, India

<sup>c</sup> Department of Materials Engineering, Indian Institute of Science, Bangalore, India

## ARTICLE INFO

### Article history:

Received 21 September 2015

Received in revised form

30 October 2015

Accepted 2 December 2015

Available online 10 December 2015

### Keywords:

Mechanical alloying

Spark plasma sintering

High entropy alloy

Grain growth

Transmission electron microscopy (TEM)

## ABSTRACT

Nanocrystalline CoCrFeNi high entropy alloy, synthesized by mechanical alloying followed by spark plasma sintering, demonstrated extremely sluggish grain growth even at very high homologous temperature of  $0.68 T_m$  ( $900\text{ }^\circ\text{C}$ ) for annealing duration of 600 h. Mechanically alloyed powder had carbon and oxygen as impurities, which in turn led to the formation of two-phase mixture of FCC and Cr-rich carbide with fine distribution of Cr-rich oxide during spark plasma sintering. Sluggish grain growth is attributed to the Zener pinning effect from the fine dispersion of oxide, mutual retardation of grain boundaries in the presence of two phases, and sluggish diffusivity because of cooperative diffusion of multi-principle elements.

© 2015 Elsevier B.V. All rights reserved.

## 1. Introduction

Nanostructured materials are of fundamental importance and are also deployed in various ambient temperature applications due to their superior properties [1]. Quite often than not, its high surface to volume ratio is intentionally exploited in technological applications. However, they are prone to grain growth even at moderate homologous temperatures ( $<0.4 T_m$ ) [2–5], and thus they do not find applications at these temperatures. Consequently, retaining their nanocrystallinity at high homologous temperatures ( $>0.6 T_m$ ) is a challenging problem among the research community. Fig. 1 (based on Table 1) illustrates the variation of grain growth factor ( $F = d_f/d_0$ ) normalized with homologous temperature and annealing duration, with respect to homologous temperature ( $T_h = T/T_m$ ). Please note that higher the normalized grain growth factor, more extensive is grain growth. It is clear from Fig. 1 that all the nanocrystalline grain growth studies demonstrated extensive grain growth even at temperatures  $<0.5 T_m$  except in the study by Chookajorn et al. [5], whose grain growth kinetics are 2–4 orders slower than all other studies.

Thus, understanding the grain growth kinetics at  $>0.6 T_m$  is quite interesting and challenging study. Solute drag, pore drag, and Zener drag are few among the effective ways in which the mobility of the grain boundaries can be inhibited, and consequently grain growth can be hindered [13,14]. Chookajorn et al. [5] utilized some of these principles to design the microstructure in bulk nanostructured W–Ti alloy by adopting a heterogeneous solute distribution to hinder grain growth.

In this connection, high entropy alloys (HEAs) are interesting materials to study grain growth kinetics since simple solid solutions form with multi-principle elements, and also due to their sluggish diffusion [15–17]. Thus, intuitively, one would also expect these alloys to have better stability of grains without much coarsening owing to sluggish diffusion associated with multi-principle elements. However, grain growth studies of HEAs are very limited [11,12] as shown in Table 1, and the reported studies are on microcrystalline HEAs. Thus, the objective of the present work is to investigate the grain growth of nanostructured HEAs, synthesized by mechanical alloying (MA) and spark plasma sintering (SPS), at higher homologous temperatures  $>0.6 T_m$ . Based on our insights from previous study on densification [18], CoCrFeNi was chosen for the grain growth studies in the present work.

\* Corresponding author.

E-mail addresses: [ravi.sankar@iitm.ac.in](mailto:ravi.sankar@iitm.ac.in), [raviskottada@gmail.com](mailto:raviskottada@gmail.com) (R.S. Kottada).

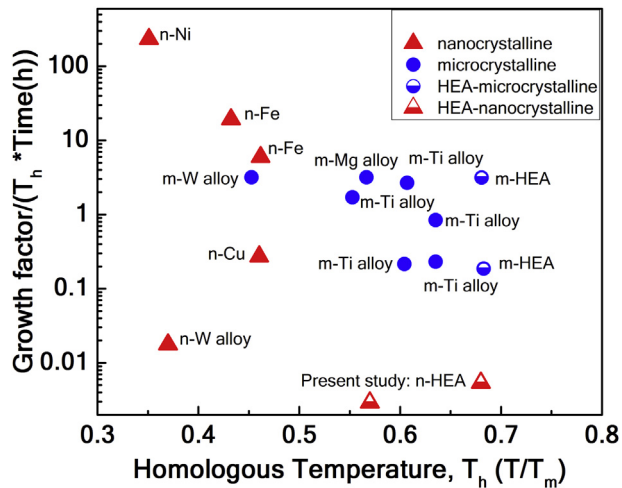


Fig. 1. Normalized grain growth factor Vs homologous temperature summarizing the present study and relevant previous studies on grain growth. [n indicates nanocrystalline materials, m indicates microcrystalline materials].

## 2. Experimental materials and procedures

Complete details on processing of nanocrystalline CoCrFeNi HEA was reported elsewhere [18]. Briefly, mechanical alloyed powders after milling for 15 h were subjected to spark plasma sintering at 900 °C for 5 min in vacuum at a constant pressure of 50 MPa. Fully dense SPS sample was heat treated in tubular furnace at 700 °C and 900 °C for 600 h (i.e. 25 days) with a break at regular intervals (24 h + 48 h + 72 h + 96 h + 120 h + 240 h), and was cooled in open air. TEM studies were carried out using FEI-Tecnai G2 F30 TEM. Elemental maps were acquired using STEM-EDS set up. High Angle Annular Dark Field (HAADF) detector was used for the imaging in mass-thickness contrast mode. More than 125 grains were counted in each phase for calculating the grain size using a linear mean intercept method from the TEM images using an open source software ImageJ.

## 3. Results

### 3.1. Phase evolution

The XRD pattern of as-milled, as-sintered, and as-heat treated (900 °C for 600 h) samples are shown in Fig. 2a. Major FCC phase with minor BCC phase were observed on milling Co, Cr, Fe, and Ni elemental powders for 15 h. After SPS, major FCC phase was retained, however BCC phase disappeared with the formation of secondary phases: Cr<sub>7</sub>C<sub>3</sub> and Cr<sub>2</sub>O<sub>3</sub>. Detailed phase evolution in CoCrFeNi alloy during MA and annealing were discussed elsewhere [18]. Formation of carbide and oxide are attributed to carbon/oxygen contamination of the MA powder during milling. Interstitial elements like carbon and/or oxygen as impurities are reported in many alloys synthesized by MA because of process controlling agent or the milling medium used [19,20]. Carbon and oxygen estimated in the as-milled powder using LECO analyser were 1.2 and 1.3 wt.%, respectively. No change in the phase structures was observed when the sintered compact was heat treated at 900 °C for 600 h. This indicates extraordinary thermal stability of the phases formed after SPS.

### 3.2. Microstructural characterization

Bright-field TEM image of as sintered CoCrFeNi (Fig. 2b)

indicates three types of grain morphology: i) faceted grains-A, ii) faulted grains-B, and iii) fine precipitates-C, and are consistent with three phases observed in the XRD pattern (Fig. 2a). The finer precipitates can be seen distributed randomly along the grain boundary and within the grains of both faceted and faulted grains. The SAD pattern acquired from faceted grain can be indexed in terms of [011] zone axis of FCC, and SAD pattern acquired from faulted grain can be indexed in terms of [22-3] zone axis of orthorhombic Cr<sub>7</sub>C<sub>3</sub>. It is also well documented in the literature that presence of many faults is a typical characteristic nature of Cr<sub>7</sub>C<sub>3</sub> [21].

The STEM-EDS elemental maps of as-sintered sample (Fig. 3) clearly suggest that the smaller precipitates are Cr–O rich, faceted grains are Cr depleted, and faulted grains are Cr–C rich. In Cr depleted grains, Co, Fe, and Ni are distributed evenly, whereas, Fe, Co, and Ni are distributed in the decreasing order in Cr rich grains. Distribution of carbon is more prominent in Cr rich grains than in Cr depleted grains or Cr–O rich precipitates. Based on the elemental mapping and SAD pattern, Cr depleted grains can be attributed to FCC phase, Cr–C rich grains can be attributed to Cr<sub>7</sub>C<sub>3</sub> phase, and Cr–O can be attributed to Cr<sub>2</sub>O<sub>3</sub> phase as also observed in the XRD pattern. Thus, the microstructure can be visualized as a composite microstructure of FCC and Cr-rich carbide phase with random dispersion of Cr-rich oxide precipitates. Although the carbide and oxide formation were due to contamination, oxide was observed as fine precipitates ( $\approx$ 30 nm) whereas carbide was observed with grain size of  $\approx$ 140 nm, which is almost equivalent to FCC phase with grain size of  $\approx$ 120 nm. This indicates that the formation of oxide and carbide are distinctly different. Based on the structure obtained after MA, we speculate that the minor BCC transforms to carbide whereas the oxide nucleates as a fine precipitate during sintering of MA powders. Transformation of minor BCC phase to carbide phase was corroborated with thermal analysis and in-situ high temperature XRD in our previous study [18]. Please note that the second phase was interpreted as sigma phase in our previous publications [18,22] due to lack of access to advanced characterization facilities, however, our present TEM studies and an independent atom probe tomography studies [23] conclusively establish it to be a carbide phase.

All three types of grains are clearly visible in STEM images of both as-sintered and heat treated sample (Fig. 4), which corroborate the excellent phase stability as evident from XRD pattern. A little increase in size of oxide precipitates, FCC grains, and carbide grains after heat treatment was observed. Average grain size (FCC + Carbide) in as-sintered and heat treated condition (900°C-600h) were  $130 \pm 40$  nm and  $258 \pm 75$  nm, respectively. The log normal distribution of grain size in as-sintered condition and after heat treatment suggests the characteristics of normal grain growth (Fig. 4). The ratio of maximum grain size to the median grain size of both FCC grains and carbide grains is  $<3$ , which also implies the characteristics of normal grain growth.

Comparison of the present study with previous studies is illustrated in Fig. 1 and Table 1. It is clear that the normalized grain growth factor of the present study is much lower than any other grain growth studies published so far, suggesting a superior grain growth resistance. It is also more interesting to note that our HEA alloy is much more resistant to grain growth even at high homologous temperatures  $>0.6T_m$ . Further, it is quite surprising that in spite of being a nanocrystalline alloy, its grain growth resistance is outstanding as compared to microcrystalline alloys. Besides, in another experiment on the same alloy, grain growth was observed to be almost negligible when it was heat treated at 700 °C (0.56  $T_m$ ) for 600h (i.e. 25 days). Average grain size (FCC + Carbide) in as-sintered and heat treated at 700 °C for 600h were  $130 \pm 40$  nm and  $125 \pm 30$  nm, respectively (Fig. 5). Also, this CoCrFeNi alloy with

Download English Version:

<https://daneshyari.com/en/article/1606649>

Download Persian Version:

<https://daneshyari.com/article/1606649>

[Daneshyari.com](https://daneshyari.com)